A MODIFIED DODGE ALGORITHM FOR THE PARABOLIZED NAVIER–STOKES EQUATIONS AND COMPRESSIBLE DUCT FLOWS

C. H. COOKE*

Department of Mathematical Sciences, Old Dominion University, Norfolk, Virginia 23508, U.S.A.

AND

DOUGLAS M. DWOYER†

NASA, Langley Research Center, Hampton, Virginia 23665, U.S.A.

SUMMARY

A revised version of Dodge's split-velocity method for numerical calculation of compressible duct flow has been developed. The revision incorporates balancing of mass flow rates on each marching step in order to maintain front-to-back continuity during the calculation. The (chequerboard) zebra algorithm is applied to solution of the three-dimensional continuity equation in conservative form. A second-order A-stable linear multistep method is employed in effecting a marching solution of the parabolized momentum equations. A chequerboard iteration is ued to solve the resulting implicit non-linear systems of finite-difference equations which govern stepwise transition. Qualitive agreement with analytical predictions and experimental results has been obtained for some flows with well-known solutions.

KEY WORDS   Modified Dodge Algorithm   Parabolized Navier–Stokes   Computational Fluid Dynamics   Low Speed Flow   Channel Flow   Zebra Algorithm   Mass Balancing

INTRODUCTION

It has been said that the full Navier–Stokes equations represent the ultimate mathematical model upon which to base numerical algorithms for predicting flows of practical significance. However, even with the advent of the so-called vector computers with vast virtual memory and quadrupled processing speeds, extant numerical and computational difficulties are sufficient to merit a search for simpler mathematical models and less complicated numerical methods which can still provide useful solutions to problems of interest. Thus, considerable analysis and numerical experiment has been devoted to the exploitation of parabolized marching methods for flow prediction. References 1 to 7 represent a perhaps typical but by no means exhaustive sampling of the available literature on this subject.

The parabolized marching methods are somewhat more general in application than the classical boundary-layer approach, since transverse pressure gradients are not disregarded and, in some cases, upstream influences can be transmitted through the pressure field.

---

* Professor.
† Aerospace Technologist.

However, the basic assumption that streamwise viscous diffusion can be neglected restricts application to flows with a primary flow direction, limited upstream influence, and which may exhibit, at worst, crossplane recirculation. Unfortunately, in subsonic and transonic wind-tunnel flows, the elliptic upstream influence can be a significant factor in the flow dynamics; hence, interest arises in simpler mathematical models which permit this interaction. A case in point has been the development of Dodge's velocity splitting method, which allows global propagation of influence through the pressure field and which has met with successes in both unconfined compressible and confined compressible flows.[7-10] However, the method is not yet fully proved.

In this paper we shall be concerned with the application of a compressible formulation of Dodge's split velocity technique[9] to the calculation of developing flow in a square duct. The original method has been revised to effect constant mass flow rate on each transverse plane while marching down the channel. Parabolized momentum equations are employed. However, a fully elliptic pressure field is allowed by the iterative manner in which the solution of the continuity equation is coupled into the calculation procedure. Application of the presently developed computer algorithm is restricted to subsonic flow. It could readily be altered to allow transonic calculations through modification or replacement of the algorithm used to solve the conservative continuity equation.

Computational simplicity as well as numerical stability is achieved in marching the momentum equations with an A-stable[11] implicit linear multistep method, the equations of which are iteratively solved at each step by employing chequerboard successive overrelaxation. Although this solution procedure may be considered expensive, the presence of quadratic as well as higher order non-linearities in the parabolized momentum equations requires that some iteration be employed to improve accuracy. As an extra benefit, the wide-ranging stability of the resulting marching equations appears well worth the cost.

Finally, the peak efficiency of the methods developed is undoubtably best realized on the computer system for which it has been designed, namely, the Cyber 203. For such machines, a numerical algorithm must effectively exploit the array-processing capabilities; otherwise, methods which are not highly vectorizable misuse the available computing potential and can result in quite ordinary processing speeds. The explicit nature of the chequerboard algorithm yields a highly vectorizable method ideally suited for the array processor.

In certain parabolized marching schemes for confined flow,[1] it has been the practice to decouple streamwise and transverse pressure gradients. Some argue[12] that this is necessary in order to obtain meaningful physical solutions with parabolized equations. Although results are still inconclusive, computational experience gained in the current research appears to support this belief. Weak, but not total, uncoupling of the streamwise pressure gradient has appeared necessary, although this may stem from the manner in which local continuity of mass flow is enforced.

As noted by Patanker and Spalding,[6] the description of a numerical procedure for solving the Navier–Stokes equations can have two aims, which are seldom possible or desirable to accomplish simultaneously. The first aim is to convey to the reader an understanding of the major principles in sufficient detail that someone with a background in the area could improvise the remainder for himself. The second aim is to present the particular equations and all approximations employed to a degree that the computational experiment could be identically reproduced. However, the second mode requires such proliferation of detail that smooth reading is impeded and understanding is inhibited. Therefore, the first aim has been chosen for the present paper, and this will be attempted in the following sections.

PARABOLIZED GOVERNING EQUATIONS

The non-dimensional Navier–Stokes equations for compressible steady flow with which we shall be concerned are presented below.

Continuity

$$\nabla . \rho \bar{w} = 0 \tag{1}$$

Momentum

$$\rho(\bar{w} . \nabla)\bar{w} = -\nabla P - \nabla \times \frac{\mu}{Re} \nabla \times \bar{w} + \nabla \frac{4}{3} \frac{\mu}{Re} \nabla . \bar{w} \tag{2}$$

Energy

$$T = T_0 - \tfrac{1}{2}\bar{w}^2 \tag{3}$$

Here, for flow in ducts with non-conducting walls, the usual energy equation has been replaced by the algebraic constant total temperature relation (3). The constitutive relations are

$$P = \frac{\gamma - 1}{\gamma} \rho T \tag{4}$$

and the viscosity approximation

$$\mu = (\gamma - 1)T \tag{5}$$

For subsonic flow the governing equations are elliptic. However, a common approximation used to parabolize these equations[1,2] is obtained by neglecting streamwise diffusion terms in equation (2). With the exception of the entry region, the approximation is considered valid for flow in channels whose lengths are large compared to half-width.[2] Perhaps it should be remarked that when Dodge's method is applied in obtaining numerical solutions of these equations the approximation is only a partial parabolization, since the pressure field is obtained from an elliptic boundary value problem. This, of course, allows global propagation of disturbances, through the pressure field and the iteration process.

DODGE'S METHOD

Introduction

In Dodge's method, the total velocity vector $\bar{w}$ is arbitrarily decomposed as a sum of rotational and irrotational parts:

$$\bar{w} = \nabla \phi + \bar{u} \tag{6}$$

where ϕ is a scalar potential. Pressure is hypothesized to depend solely upon the irrotational velocity according to the isentropic relationship

$$P = P_0 \left(\frac{1 - \nabla \phi^2}{2T_0} \right)^{\gamma/\gamma - 1} \tag{7}$$

However, density is decomposed as the sum of a viscous contribution ρ_v and an isentropic contribution ρ^*:

$$\rho = \rho_v + \rho^* \tag{8}$$

where

$$\rho^* = \rho_0 \left(\frac{1 - \nabla \phi^2}{2T_0} \right)^{1/\gamma - 1} \tag{9}$$

Substituting equations (6), (7), and (9) in equations (1) and (2) leads to the so-called split equations

$$\nabla \cdot \rho \nabla \phi = -\nabla \cdot \rho \bar{u} \tag{10}$$

and

$$\rho(\bar{w} \cdot \nabla)\bar{w} - \rho^*(\nabla \phi \cdot \nabla) \nabla \phi + \nabla \times \left(\frac{\mu}{Re} \nabla \times \bar{w} \right) - \nabla \left(\frac{4}{3} \frac{\mu}{Re} \nabla \cdot \bar{w} \right) = 0 \tag{11}$$

Equations (10) and (11) are to be iteratively solved: equation (10) with a 3-D relaxation method for elliptic equations, following which the parabolized version of equation (11) is marched downstream by employing a chequerboard iteration to solve an implicit system of equations at each step. A synopsis of the iteration procedure is now presented.

Overview of iteration procedure

(1) Determine a suitable initial pressure distribution P_0 by estimating a global ϕ distribution. In this investigation, pressure on the first pass is assumed to be a function of only streamwise displacement, and a mass-balancing operation establishes the initial pressure field.
(2) Employing the current pressure field, march a parabolized version of equation (11) down the duct, simultaneously storing the right-hand side of equation (10). (See also equation (17)).
(3) Solve equation (10) (or equation (17)) to obtain an updated pressure field.
(4) Repeat the computational pass consisting of steps (2) and (3) until sufficient passes and a converged pressure field are obtained.

Dodge's method revised

Dodge[9] reports problems arising from adjustment of front-to-back continuity requirements with an iteration which is similar to that previously outlined. It is expected that this slow convergence stems from incomplete satisfaction of the continuity equation which could, for example, be solved after the momentum march terminates in some form such as

$$\nabla \cdot \rho_n \nabla \phi_n = -\nabla \cdot (\rho \bar{u})_{n-1} \tag{12}$$

This is in contrast to the usual parabolized marching methods, for which both mass and velocity variables are updated at each marching step.

Physically, in order to maintain continuity in a channel flow, the mass flow rate

$$\omega = \iint \rho \left(\frac{\partial \phi}{\partial \chi} + u \right) dy \, dz = \iint \rho \bar{w}_{normal} \, dy \, dz \tag{13}$$

must remain constant at each transverse plane. However, in Dodge's (unrevised) method this

provision is only weakly incorporated through equation (10), which is solved globally upon termination of a marching pass. Thus, poor satisfaction of mass balancing during the momentum marching process is only to be expected, as numerical experimentation indicates.

Consequently, the Dodge technique is to be revised in a manner which alleviates this difficulty. This is accomplished by expressing ϕ as

$$\phi(x) = \int_0^x g(\xi) \, d\xi + \tilde{\phi}(x, y, z) \tag{14}$$

with $g(x)$ iteratively chosen to balance mass flow rate at location x.

In the usual Dodge method, pressure gradients on pass n are chosen from the equation

$$\frac{\partial P}{\partial x_i} = -[\rho^*(\nabla\phi \cdot \nabla) \nabla\phi]_i^n \tag{15}$$

In the revised version pressure gradients are allowed to develop during the mass balancing iteration according to the equations

$$\frac{\partial P^{n,k}}{\partial x} = -\rho_{k,n}^*(g^k g_x^k + \phi_y^n \phi_{xy}^n + \phi_z^n \phi_{xz}^n) \tag{16}$$

$$\frac{\partial P^{n,k}}{\partial y} = -\rho_{k,n}^*(g^k \phi_{xy}^n + \phi_y^n \phi_{yy}^n + \phi_z^n \phi_{yz}^n) \tag{17}$$

$$\frac{\partial P^{n,k}}{\partial z} = -\rho_{k,n}^*(g^k \phi_{xz}^n + \phi_y^n \phi_{yz}^n + \phi_z^n \phi_{zz}^n) \tag{18}$$

where the balancing iteration on mass flow rate is

$$g^{k+1} = g^k - \left[\omega - \int\int (\rho w_{\text{normal}})^k \, dy \, dz\right] \bigg/ \int\int \rho^k \, dy \, dz \tag{19}$$

and g_x is obtained by second order backward differencing.

First attempts at choosing $\tilde{\phi}$ as a solution of

$$\nabla \cdot (\rho \, \nabla\tilde{\phi})_n = -\nabla \cdot (\rho\bar{u})_{n-1} - \frac{\partial}{\partial x} (\rho g)_{n-1} \tag{20}$$

were unsuccessful, due largely to the fact that the elliptic–hyperbolic transition point of (20) can differ markedly from the physical. This difficulty is largely alleviated, although not to totally circumvented, by choosing ϕ from the equation

$$\nabla \cdot (\rho \, \nabla\phi)_n = \nabla \cdot (\rho u)_{n-1} \tag{21}$$

whose transition point more closely approximates the physics of the flow. Clearly, choice of g does not affect mixed derivatives, or cross plane derivatives of ϕ.

The procedure outlined represents a weak decoupling of the streamwise pressure gradient, since the g terms are the dominant contributions, and since these contributions are determined from local plane-to-plane continuity considerations, somewhat independently of the output from the global continuity equation (equation (21)) on the previous pass.

NUMERICAL ANALYSIS

The algorithm deemed most efficient for numerically solving equation (21) on the array-processing computer is the zebra algorithm of South et al.[13] This 3-D relaxation technique is

in some respects similar to the hopscotch method of Gourlay.[14] In equation (21) central differences are applied to all derivative terms. Variables in plane i are updated in chequerboard fashion, plane by plane in a downstream sweep, using already updated values at plane $i-1$ and old iteration values in plane $i+1$. Iterative repetition of downstream sweeps is used to converge the field, with a relaxation parameter employed to speed convergence.

A second-order accurate, implicit linear multistep method is used on equation (11) to march in the stepwise direction. The implicit equations are iteratively solved using a chequerboard successive overrelaxation scheme, with mass balancing built in as previously described. Streamwise derivatives are backward differenced second-order accurate, whereas derivatives in the (transverse) cross-plane are approximated second-order using central differences. A prediction of form

$$f_i = 2f_{i-1} - f_{i-2} \tag{22}$$

is used to initially estimate a velocity variable in plane i. The chequerboard method is then employed on the differenced counterpart of equation (11) to update variables in plane i in two cycles, with values updated on cycle 1 fed into the succeeding cycle. This two-cycle update process is iterated, employing equations (16)–(19) to alter the flow speed and pressure gradients until a balance in mass flow is achieved.

DEVELOPING FLOW IN A STRAIGHT DUCT

The revised method of Dodge has been employed to develop a finite-difference numerical model for three-dimensional viscous flows in confined regions. For boundary-layer resolution, the capability to allow individual co-ordinate stretching in each co-ordinate direction has been incorporated. The method so developed has been programmed using the SLI vector language for the Cyber 203 array processor, and appears debugged. The 32-bit half-word option of SLI has been employed in programming the zebra relaxation algorithm for solving equation (21), whereas 64-bit full-word arithmetic is used in programming the chequerboard marching algorithm. The program has been tested by application to the problem of computing the steady developing flow in a straight duct (see Figure 1). Boundary conditions for the problem are now given.
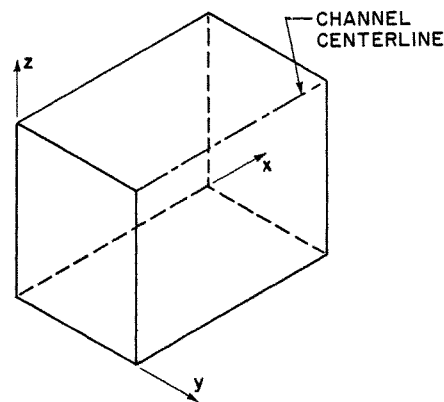

Figure 1. Quarter channel computational domain

Boundary conditions

Inflow. $T = T_0 - \frac{1}{2}u_i^2$
specified velocity profiles, $\bar{W}_0 = \bar{H}(y, z)$,
$\rho_i = R(y, z)$, $P_i = $ constant
$\phi_x(0, y, z) = g(0) = g_0$

Duct walls. Velocity no slip, $\phi_n = 0$, $T = T_w$, $\rho = \rho_w$

Outflow. ρ_v extrapolated, $\phi = \phi_m$, g_m extrapolated

Artificial barriers. The computational domain is taken to be one quarter of the total duct cross-section, and symmetry conditions are applied at the two resulting (non-wall) artificial barriers. Here the normal velocity component vanishes together with normal derivatives of ϕ and the other velocity variables. The variables P and T, of course, depend on ϕ and velocity at these boundaries. However, for constant total temperature, vanishing normal derivative in T, ρ is the natural boundary condition.

COMPUTATIONAL RESULTS

Introduction

An assessment of approximation error inherent in numerical solutions of parabolized flow models computed with the revised Dodge's method has been undertaken. This has been accomplished for certain flows whose solutions have been either analytically or experimentally determined and which are available for comparison with numerical results.

Two-dimensional channel flow, Re = 100

Numerical solutions for two-dimensional, low Mach number $(M \leq 0.05)$ flow in a straight channel (see Figure 2) have been computed, employing a uniform mesh of $17 \times 17 \times 100$ nodes. The development of the normalized centreline velocity component V_x/U characterizing the two-dimensional channel and the corresponding results of Goldstein and Kreid[15] for three-dimensional flow in a square duct are compared in Figure 2. For the fully developed case Schlicting[16] gives a limiting value $V_x/U = 1.52$. The corresponding maximum value from
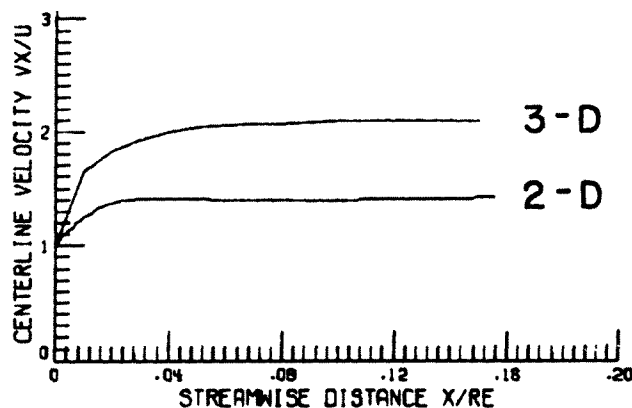

Figure 2. Comparison of normalized centreline velocity development for two and three-dimensional channel flow
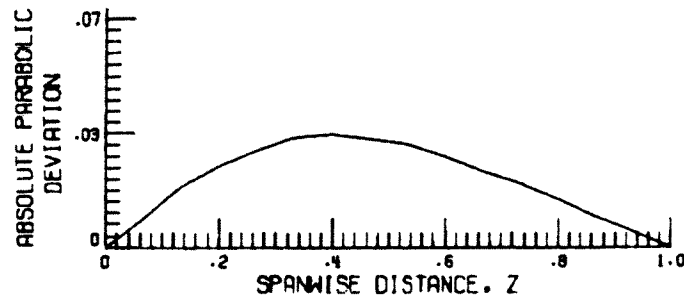
Figure 3. Deviation from a parabolic profile of the streamwise velocity component at outflow—two-dimensional flow

the computational results of Figure 2 is $V_x/U = 1\cdot425$. This represents a relative error of six per cent or less, depending upon how fully developed the numerically calculated flow is considered to be. One should perhaps also bear in mind that Schlicting's results come from matched asymptotic expansions, which are in themselves approximate methods. Figure 3 exhibits typical spanwise deviation from a parabolic profile characteristic of V_x at numerical full development. The maximum error is again on the order of five or six per cent.

Three dimensional duct flow, Re = 100

A $32\times32\times100$ mesh has been employed to compute low Mach number, three-dimensional flow in a square duct. Streamwise variation in centreline velocity component V_x and pressure P are shown in Figures 4 and 5. A comparison between numerical calculations for V_x/U and the corresponding experimental results of Goldstein and Kreid[15] is shown in Figure 6. Comparative fully developed values for V_x/U at centreline for the two cases are $1\cdot93$ and $2\cdot10$. Including grid stretching in the calculation improved the former value to $1\cdot9725$. This again represents a relative error in the vicinity of six per cent.

Figures 7–9 show numerical performance indicators which trace the convergence history of a typical calculation. Here two kinds of outflow boundary conditions for solution of the elliptic velocity potential equation have been tested. For the calculation represented by Figure 9, a Dirichlet condition was applied. Although a seemingly more rapid, non-oscillatory convergence history is observed, distortion is streamwise velocity and pressure
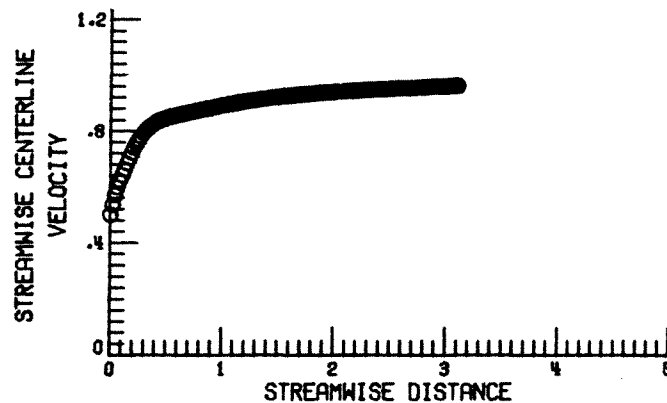

Figure 4. Flow development for streamwise velocity component—three-dimensional duct flow
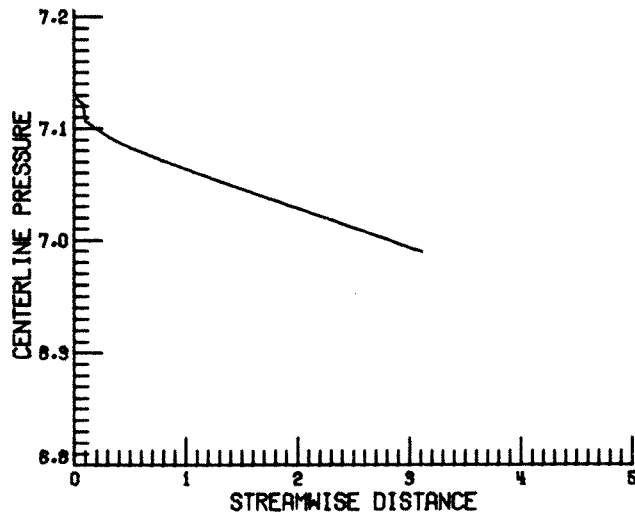
Figure 5. Streamwise development for centreline pressure—three-dimensional duct flow

profiles near the channel exit accompanied its application. A Neumann boundary condition appeared to eliminate these non-physical distortions, but at the misfortune of a more sluggish, oscillatory, convergence history (see Figures 7 and 8). The Neumann condition was chosen for the calculations heretofore discussed.

Figures 10 and 11 show characteristics of the exit crossflow and boundary-layer profiles for the streamwise velocity component. In calculating the fully developed crossflow of Figure 11, a channel length of $X_m = 12$ units with a coarse mesh having 144 downstream nodes was employed. The sink irregularity near channel centreline in Figure 10 was observed to move closer to channel centre as the length increased, and appeared to have coalesced with it in the calculation of Figure 11. The tendency of the core flow to be directed towards channel centreline (see Figures 10 and 11) is in qualitative agreement with the theoretical predictions of Rubin[4] concerning the asymptotic behaviour of duct crossflow.
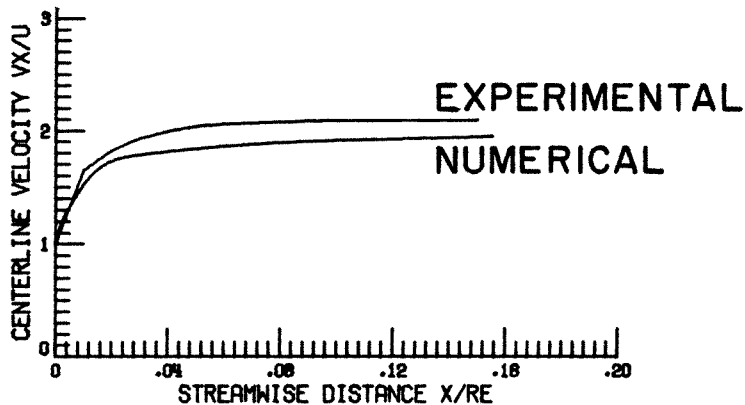

Figure 6. Experimental versus computed development for streamwise velocity component—three-dimensional duct flow
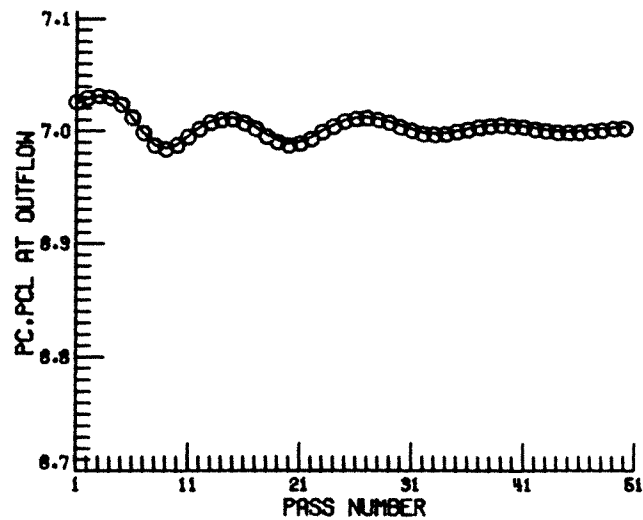
Figure 7. Iteration history, corner and centreline pressure at the outflow—Neumann condition

CPU time

A computer code for the revised version of Dodge's method employs the SLI-language for the Cyber 203 version of the CDC-STAR computer. With a $17 \times 17 \times 196$ mesh, measured time for program execution was found to average $2 \cdot 3 \times 10^{-4}$ computer resource units (CRU's) per node per model equation per pass. (This assumes only four model equations, since the energy equation was replaced with an algebraic relationship.) A pass consisted of marching the momentum equations once down the duct, iteratively solving an implicit system for velocity propagation at each streamwise station using a chequerboard scheme, and then finding the zebra solution of the three-dimensional velocity potential equation. When measuring performance in CPU seconds per node per model equation per pass, the corresponding figures becomes $4 \cdot 14 \times 10^{-4}$.
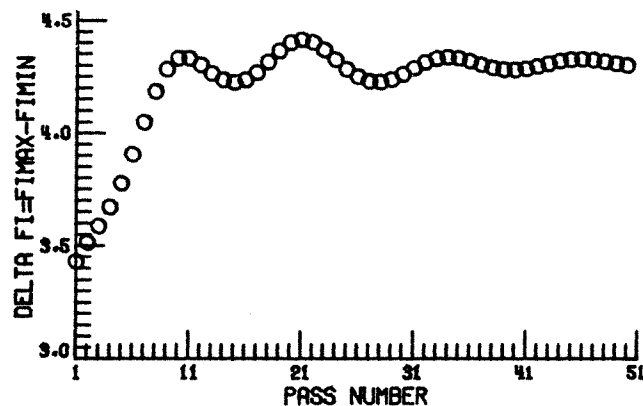

Figure 8. Iteration history, streamwise increment in velocity potential—Neuman condition at outflow
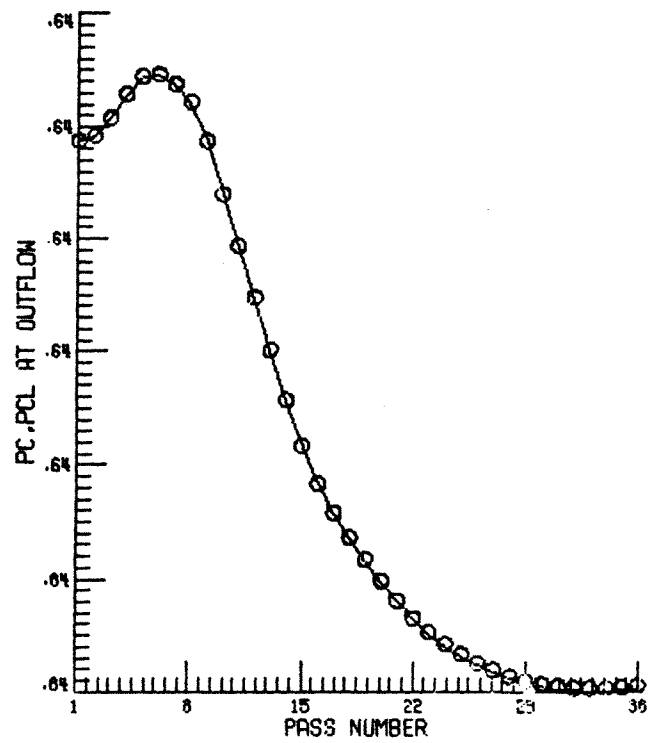
Figure 9. Iteration history, corner and centreline pressure at outflow—Dirichlet condition on velocity potential
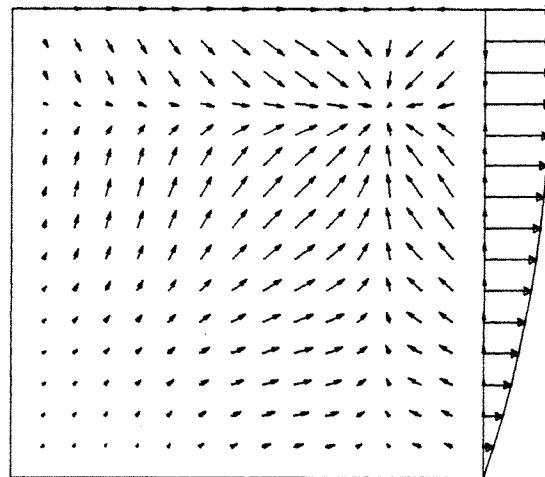

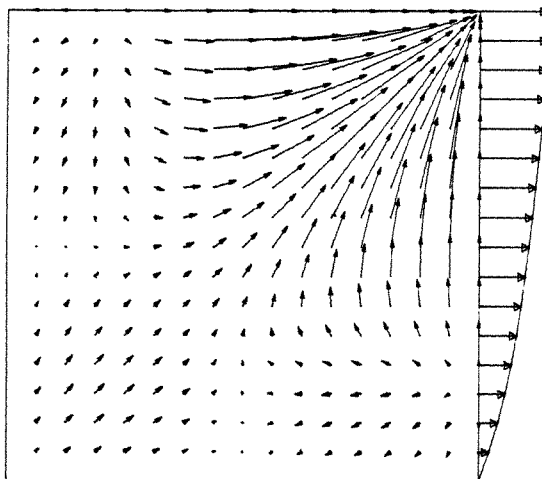Figure 10. Crossflow and boundary-layer profile for streamwise velocity component at channel exit, $Re = 100$, $X_m \approx 3 \cdot 0$

Figure 11. Fully developed exit flow, $Re = 100$, $X_m = 12 \cdot 0$

SUMMARY AND CONCLUSIONS

A revised version of Dodge's velocity-split method for numerical solution of compressible confined flow has been developed. Numerical results from test calculations for low Reynolds number flow appear encouraging. In particular, qualitative but not wholly satisfactory quantitative agreement between present calculations and analytical predictions of Schlicting[16] and Rubin,[4] together with experimental measurements of Goldstein and Kreid,[15] has been achieved.

However, the method is by no means fully understood or exhaustively and conclusively tested. A curious feature of the present approach is the need for weak decoupling of the streamwise pressure gradient, found necessary in order to achieve a convergent numerical solution. However, Spalding[12] alleges that to obtain meaningful solutions using parabolized equations such a full decoupling is necessary. Further, Briley[1] reports successful and quantitatively accurate calculations obtained with an algorithm which incorporates this practice. Be that as it may, in this study convergence problems, first manifested by irregularities in the entrance region of the duct, were observed, but disappeared upon weakly decoupling the streamwise pressure gradient. Even so, the numerical calculations appeared overly sensitive to the treatment of the inflow, a characteristic of parabolized duct flows perhaps hinted at by Briley's suggestion of shutting off the crossflow in the first few steps of the march.[1] Rubin[4] alleges that the full Navier–Stokes equations are required to properly model entry region flow. Hence, the failure to properly smear errors in this region may have been the root problem, assuming such errors can be widely propagated, either upstream or down, in solving the elliptic velocity potential equation.

In addition to cases previously recorded, a convergent numerical solution for $Re = 1000$ flow in a duct of length $X_m = 6$ has been achieved. However, for satisfactory calculations at high Reynolds numbers, or for longer ducts, a more powerful adaptive grid capability than is to be afforded by simple stretchings in individual co-ordinates appears necessary. In duct flow the driving mechanism is streamwise boundary-layer growth and concomitant flow acceleration in the core, with the induced crossflow strongest away from the walls. Hence, as the flow develops near-wall gradients decrease, or spread in extent, while core gradients

grow. For high Reynolds numbers the result is that a grid system with a simple stretching mechanism set to capture entry region boundary layers is likely to become insufficient for resolving the more complex global patterns which emerge as the flow develops. Since boundary-layer thickness is thought to grow proportional to $(x/Re)^{1/2}$, it appears that the ideal grid should adaptively relax near-wall clustering in some such fashion.

The revision of Dodge's method reported herein as regards mass balancing is new, although classical in its physical origins and used previously with many other computational schemes. For flow in a straight duct it appears to be highly useful. However, the original intent of this investigation of Dodge's method was to discover its possible utility as a tool for solving the slotted wind-tunnel problem, where it was felt that the upstream influence permitted by the elliptic velocity potential equation would be highly desirable. This could well be so, were the method found workable without resort to the mass-balancing stratagem. However, it is not felt that the present formulation with added on mass-balancing can be useful. This is because of the possibility of large pressure variations from tunnel to plenum, which would make the simultaneous balancing of mass on a plane extending over two essentially disparate channels with limited communication through the slots unfeasible, as balancing over the entire region would have to be accomplished through tuning the streamwise pressure gradient.

Possibly the most successful innovation of this investigation is the use of the chequerboard iteration as a tool for solving at each marching plane the implicit finite-differenced momentum equations. It should be noted that the chequerboard algorithm used is different from either the hopscotch method used by Rudy[17] or the recent hopscotch innovation of Greenberg.[18] In both cases, iteration is not practised in solving an implicit system; hence, the well-known inconsistency of the hopscotch method becomes significant, at least during the transient calculation. In the present case no transient exists, since the steady equations are being solved. The inconsistency of the usual hopscotch method is thus hard to bear, as it could head to problems in solution accuracy.

LIST OF SYMBOLS

C_{p}, C_{v}	specific heats
P	static pressure
ρ	density
$\bar{w}$	three-dimensional velocity vector
μ	viscosity
Re	Reynolds number, $\dfrac{\rho_0 a_0 D}{\mu_0}$
γ	C_{p}/C_{v}
T	temperature
$T_0, p_0, \rho_0, a_0, \mu_0$	reservoir values for temperature, pressure, density, speed of sound, and viscosity
ϕ	scalar potential
α	relaxation of parameter
D	channel half-width
M	Mach number
V_x/U	ratio of channel streamwise velocity component to entrance value

REFERENCES

1. W. R. Briley, 'Numerical method for predicting three dimensional steady viscous flow in ducts', *J. Comput. Phys.*, **14** (1), 1974.
2. G. A. Carlson and R. W. Hornbeck, 'A numerical solution for laminar entrance flow in a square duct', *J. Appl. Mech.*, 25–30, March (1973).
3. R. Chilukuri and R. H. Pletcher, 'Numerical solutions to the partially parabolized Navier–Stokes equations for developing flow in a channel, *Numerical Heat Transfer*, **3**, 169–188 (1980).
4. S. G. Rubin, P. K. Khosla and S. Saari, 'Laminar flow in rectangular channels', *Computers and Fluids*, **5**, 151–173 (1977).
5. Richard S. Hirsh, 'Numerical solution of supersonic three-dimensional free mixing flows using the parabolic-elliptic Navier–Stokes equations', *NASA TN D-8195*, November 1976.
6. S. V. Patanker and D. B. Spalding, 'A calculation procedure for heat, mass, and momentum transfer in three-dimensional parabolic flows', *Int. J. Heat and Mass Transfer*, **15**, 1787–1806 (1972).
7. R. R. Cosner, 'Fast Navier–Stokes solution of transonic flowfield about axisymmetric afterbodies', *AIAA-80-0193, AIAA 18th Aerospace Sciences Meeting*, Pasadena, Calif., 14–16 January, 1980.
8. P. R. Dodge, 'A numerical method for 2-D and 3-D viscous flows', *AIAA Paper No. 76-425, 9th Fluid and Plasma Dynamics Conference*, San Diego, Calif., 14–16 July, 1976.
9. P. R. Dodge, '3-D heat transfer analysis program', *AFAPL-TR-77*, 21-2541(7), September 1977.
10. D. L. Dwoyer, 'Velocity split Navier–Stokes solution procedure for incompressible high Reynolds number external flows', *NASA TN-1655*, April 1980.
11. G. Dahlquist, 'A special stability problem for linear multistep methods', *BIT*, **3**, 27–43 (1963).
12. D. B. Spalding, 'Numerical computation of steady boundary-layers', *Proceedings, Conf. on Computational Methods and Problems in Aeronautical Fluid Dynamics*, University of Manchester, September 1974.
13. J. C. South, J. D. Keller and M. M. Hafez, 'Vector processor algorithms for transonic flow calculations', *Proc. of AIAA Fourth Computational Fluid Dynamics Conference*, Williamsburg, Va., 23–24 July, 1979.
14. A. R. Gourlay, 'Hopscotch: a fast second-order partial derivative equation solver', *J. Inst. Math. Appl.*, **6**, 375–390 (1970).
15. R. J. Goldstein and D. K. Kreid, 'Measurement of laminar flow development in a square duct using a laser Doppler flow meter', *J. Appl. Mech.*, 813–818, December (1967).
16. Herman Schlicting, *Boundary Layer Theory*, McGraw-Hill, 1960.
17. David H. Rudy, Dana K. Morris, Stanley Rubin and C. H. Cooke, 'An investigation of several numerical procedures for time asymptotic compressible Navier–Stokes equations', *NASA SP-347*, 1975.
18. J. B. Greenberg, 'Some semi-implicit hopscotch type methods for the time dependent compressible Navier–Stokes equations', *AIAA Paper 81-1022, AIAA 5th Computational Fluid Dynamics Conference*, Palo Alto, Calif., 22–23 June, 1981.